The International Journal of Advanced Manufacturing Technology
https://doi.org/10.1007/s00170-023-12160-z

ORIGINAL ARTICLE

Advantages in the production of power transmitting gears by fineblanking

Anian Nürnberger[1] · Daniel Müller[1] · Lukas Martinitz[1] · Christoph Hartmann[1] · Thomas Tobie[2] · Karsten Stahl[2] · Wolfram Volk[1]

Received: 8 May 2023 / Accepted: 11 August 2023

Abstract
Fineblanking of gears has an enormous time and cost saving potential as well as the potential to significantly reduce CO_2 emissions compared to conventional manufacturing of gears. Conventional manufacturing of gears consists of at least three steps such as milling, case hardening, and grinding. With fineblanking, only one manufacturing step is necessary. However, the load-carrying capacity regarding different gear fatigue failure modes, such as pitting or tooth root breakage, is stated significantly lower for the commonly used shear-cutting steels compared to the conventional case-hardened gears made out of high-strength hardened steels. This work shows the possibility of utilizing compressive residual stresses that are induced by the fineblanking process to increase the load-carrying capacity regarding tooth root breakage up to the level of case-carburized gears. Pinions and wheels made of S355MC (1.0976) and S500MC (1.0984) are fineblanked using parameters determined in previous works with a focus on the induction of high compressive residual stresses into the finished products. The variants are investigated regarding, e.g., cut surface characteristics, hardness, and residual stresses. For the two steels, as well as a stress relived variant, the tooth root bending strength is also determined in pulsator tests with the fineblanked pinions.

Keywords Gears · Shear cutting · Near-net-shape blanking · Fineblanking · Residual stresses · Fatigue testing · Tooth root breakage · Tooth root bending strength

1 Introduction

In conventional gear manufacturing processes of case hardened gears, shot peening as an additional refinishing step is used to induce higher compressive residual stresses, increasing the load-carrying capacity up to 50% [1]. With fineblanking high compressive residual stresses can be induced in a single manufacturing step. The height of the compressive residual stresses depends on the fineblanking process parameters, such as the die edge radius r_M as well as the sheet material. For higher strength materials higher compressive residual stresses can be induced that also have higher influence on the load-carrying capacity due to a higher residual stresses sensitivity [2]. Compared to conventional manufacturing of gears, consisting of at least three process steps (milling, case hardening, and grinding), the process of fineblanking has enormous time and cost-saving potential.

2 State of the art of fineblanking

The fineblanking manufacturing process was developed in Switzerland as early as 1923. Workpieces for mechanical precision movements used to be produced by the manufacturing process of normal cutting and then scraped to smooth the cut surfaces and ensure the required dimensional accuracy. In 1959, the industrial use of fineblanking began. The requirements for cut surface quality and dimensional accuracy could be achieved in a single operation. The previously used combination of two processes could thus be substituted [3]. The ongoing development of fineblanking enables the production of complex components with a high degree of

✉ Anian Nürnberger
anian.nuernberger@utg.de

✉ Daniel Müller
daniel.mue.mueller@tum.de

[1] Chair of Metal Forming and Casting, Technical University of Munich, Walther-Meissner-Str. 4, Garching 85748, Bavaria, Germany

[2] Institute of Machine Elements, Gear Research Center (FZG), Technical University of Munich, Boltzmannstraße 15, Garching 85748, Bavaria, Germany

Published online: 31 August 2023

functional integration. This is also made possible by combining fineblanking with other cold-forming processes such as deep drawing, bending, extrusion, coining, and flanging. [4] Fineblanking itself, which is limited to cutting out components, makes it possible to achieve cut surfaces that are smooth across the entire sheet thickness in just one stroke. In addition, very tight tolerances can be maintained in terms of dimensional and shape accuracy. Due to the high component quality that can be achieved and the possibility of combining it with forming operations, this manufacturing process is the most widely used precision-cutting process in the industrial environment [5]. Due to the high achievable quality of fineblanked parts and the cost-effectiveness of this technology, it often makes sense to replace previously finecast, sintered, forged, or even machined components with fineblanking [3]. Apart from any deburring that may be necessary, fineblanked components can be installed and their cut surface directly be used as a functional surface for transmitting forces or motions [5]. Dietrich [6] states that gears with a module of 0.2 to 10 mm can be fineblanked with a sheet thickness of 1 to 10 mm. Fineblanking is characterized by the use of a v-ring on the die and/or blankholder, a counterpunch, a very small die clearance, and cutting-edge preparation on the blanking punch and die, as shown in Fig. 1. Three independent forces (blankholder force, cutting force, and counterpunch force) act during the fineblanking process, requiring specialized fine blanking presses with primarily hydraulic or servomechanical drive concepts. Before cutting begins, one or more v-rings penetrate the sheet material and clamp the semi-finished product. The v-ring force responsible for clamping increases to a specified level and remains approximately at this level. Then, the punch, which is guided by the blankholder, penetrates the material, with the counterpunch pressing the subsequent cutout against the punch with an approximately constant force and preventing deflection of the resulting component. After the punch has penetrated the sheet metal, the blankholder strips, the stamped strip, and the component are pushed out of the die by the counterpunch [7].

No cutting impact occurs when the material is cut through, which is another process-related advantage [8]. According to VDI norm 2906, the achievable cut surface quality or functional surface quality is mainly characterized by the die roll or die roll height, the clean-cut percentage, any possible tears and tear-offs, the roughness of the clean-cut surface, the cut surface angle, the burr, the hardened area close to cut surface, and any bulging that may be present [9]. In the following, the influence of the essential quality characteristics will be discussed:

In general, the die roll height increases with increasing material thickness and decreasing material strength [10]. Likewise, the microstructure of the material influences the die roll height, too [9]. Particularly, in the case of gear teeth, the angle of the chamfer on the die cutting edge has an influence

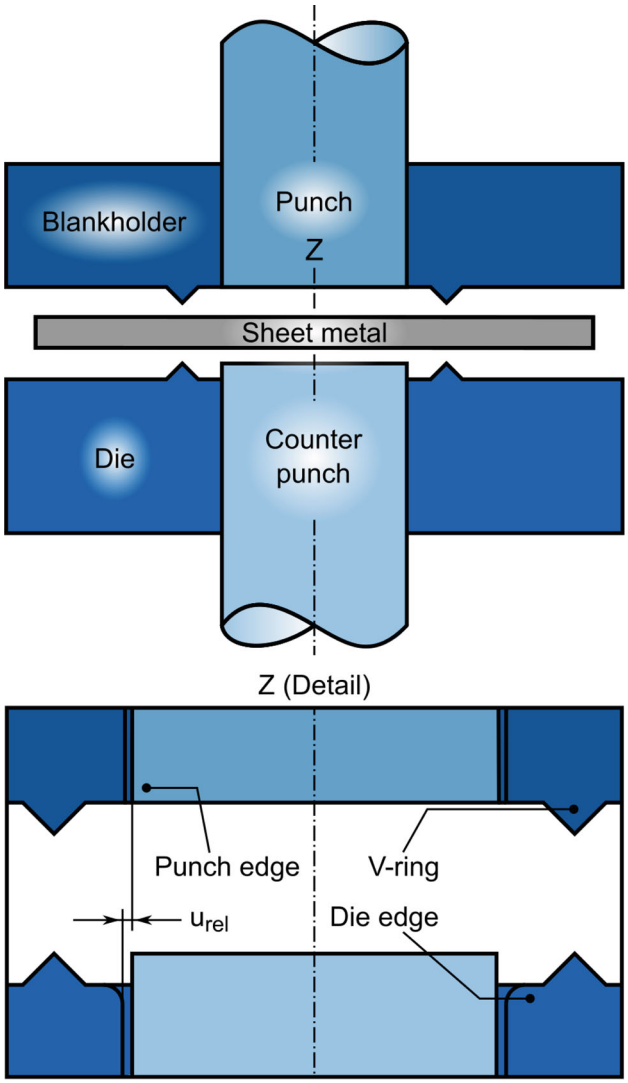

Fig. 1 Schematic of fineblanking (top) and detail (below)

on the die roll height, which increases with increasing chamfer angle. Also, the die roll height increases with decreasing gear module (gear tooth size), i.e., for gears with a module larger than 1.0 mm and then decreases again for teeth with a module smaller than 1.0 mm [11].

For exposed geometry elements, such as a tooth of a gear, in general, it is stated that as the angle for the exposed part becomes smaller and the fillet at the end becomes smaller, the die roll height increases [12]. Fuchiaki et al. [13] confirm a large influence of cutting line geometry on die roll height. Kim [14] showed on gear-like components that as the distance between the v-ring and the cutting line increases, the die roll height increases. An increase in the die clearance is also associated with increasing die roll height [15]. An increase of the clean-cut percentage is achieved by reducing the die clearance [16]. This fact is confirmed by Sahli et al. both experimentally and simulatively [17]. Regarding the

cutting line, the die clearance does not have to be constant, but can vary for difficult geometric shapes of the cut part. As a rule of thumb for the die clearance, 0.5% of the sheet thickness to be cut can be assumed [10].

Rounding or faceting of the die cutting edge also contributes to higher clean-cut percentages, decreasing material flow and in return reducing the susceptibility to cracking [5]. The use of a v-ring on the blankholder and/or die prevents a rotating material flow in the shear zone during fineblanking according to Thipprakmas, thus increasing the hydrostatic stress state and contributing to a higher clean-cut percentage [18]. Elyasi [19] concludes that increasing the v-ring angle up to 90° leads to higher clean-cut percentages. In contrast, an increasing radius of the v-ring tip has a negative effect on the clean-cut percentage, whereby it finds an optimum for the v-ring height. The same applies to the distance of the v-ring from the cutting line, whereby a negative influence on the clean-cut percentage can be observed, if the optimal distance of the v-ring from the cutting line is exceeded.

The surface roughness of the clean-cut percentage, which is measured according to [9] in the center of the sheet thickness at 90° to the cutting direction, can reach values from Rz 3 μm to Rz 15 μm. With coated active elements, Rz values in the range of 1 to 3 μm are possible. The cut surface angle or taper of the cut surface is always present on fineblanked parts, so the outer contour is slightly larger on the burr side than on the die roll side. This inclination of the cut surface increases with increasing sheet thickness and thus moves away from the ideal of 90° [9].

A burr is also always present on the fineblanked part, but the rounding or faceting on the die and a sharp punch mean that a large burr only occurs on the stamped strip, i.e., the waste [5].

Another characteristic of fineblanked components is the high hardening compared to the base hardness, which can be detected in the area of the cut surface [5]. This fact was used by Thipprakmas [20] to increase the wear resistance of sprockets. It is typical for the hardness curve to increase starting from the die roll side towards the burr side of the cutout [9]. An interesting aspect is that residual stresses occur in fineblanked components, which on the one hand can have an effect on the geometry of components and on the other hand can improve component properties. Česnik et al. [21] showed that tensile residual stresses are present on the die roll side of fineblanked components, whereas compressive residual stresses are found on the burr side. In addition, it was shown that the intended part geometry is distorted by a relaxation of the part, which takes place after leaving the tool.

Aravind et al. [22] also refer to compressive residual stresses at fineblanked holes near the die roll side.

Evidence of compressive residual stresses in the tangential and also in the axial direction at the cut surface of fineblanked disks with circular geometry, at the stamped strip, and at the cutout was provided by Stahl et al. [23]. Furthermore, it was demonstrated in a fatigue test that at comparable cutting surface parameters, comparable roughness, and comparable cutting surface hardness, higher residual compressive stresses caused by near-net-shape blanking lead to an increase of tolerable load cycles [24]. In addition, it was possible to generate high residual compressive stresses in the sheet thickness direction in the tooth root fillet even on components with very complex cutting line geometries, such as involute gears. It was also possible to adjust the residual compressive stresses in their magnitude via the value of the die radius. Likewise, high axial and tangential residual compressive stresses were generated in the tooth root of the gear [25]. The high compressive residual stresses could be exploited to increase the fatigue strength of a gear with module 4.5 mm with respect to the tooth root bending strength [26].

3 Problem formulation and solution approach

The conventional manufacturing process of gear teeth on gears made of metal usually comprises several complex, time-consuming, and expensive process steps. In addition to the cutting or milling of the tooth form, this also includes the modification of the materials' properties by means of energy-intensive heat treatment such as case hardening, followed by grinding. Depending on the application, shot peening processes are also carried out to introduce higher compressive residual stresses to increase the load-carrying capacity.

Against the background of saving energy and natural resources, but also shortening production times and costs, the fineblanking of power transmitting gears holds great potential. In order to further exploit this potential and determine future industrial application, the aim of this work is to transfer the knowledge gained in the previous works [25] and [26] to a higher strength steel in order to further increase the load-carrying capacity regarding tooth root breakage.

Therefore, the influence of the base materials strength on the resulting fineblanked gears is investigated. Specifically, the resulting residual stress states, hardness of the cut surface, geometric accuracy, and the flank load-carrying capacity are determined and compared with conventional manufacturing processes. Pinions and wheels with a module of 3 mm are manufactured by fineblanking out of the steels S355MC and S500MC. The fineblanking process parameters are selected based on extensive research, in such a way that the compressive residual stresses are as high as possible but the cut surface characteristics remain passable for the gear flanks. To further investigate the influence of the residual stresses, pinions made out of S500MC with no residual stresses are investigated regarding tooth root bending strength.

4 Experimental setup and test equipment

4.1 Materials

Fine-grain structural steels S355MC and S500MC according to the standard DIN EN 10149-2 [27] with a plate thickness of 6 mm are used for the sample production. Table 1 shows the chemical elements composition analyzed by spark emission spectrometer after the delivery of the sheet plates. In preparation for the fineblanking tests, semi-finished products with dimensions of 150 mm × 150 mm × 6 mm are cut out by laser. The blanks are then machined at the laser-cut edges to dimensions of 136 mm × 136 mm, in order to remove the heat-affected zone of the laser-cutting process. Furthermore, three unit holes, later used for positioning, were drilled into the test specimens. The basic hole in the center serves as centering for measurements, and the other two basic holes are for the exact positioning of the semi-finished products on the die. In this way, clear documentation could be ensured by means of corresponding markings. Before fineblanking, the blanks are subjected to a stress-relief annealing process to ensure a uniform initial residual stress state for the herein-performed investigations. During the temperature control, care is taken not to exceed 580 °C according to DIN EN 10149-1 [28]. Microstructural changes, in particular recrystallization, are ruled out by microstructural examination and comparison with the untreated material.

4.2 Fineblanking tools and process parameters

The fineblanking tests are carried out with a Feintool "HFA 3200 plus" fineblanking press. For fineblanking the pinion and wheel, a die, a punch, a blankholder, and a counterpunch are manufactured for each geometry. For the two materials of different strength, the adjustable process forces, i.e., v-ring force F_R and counterpunch force F_{Geg}, are calculated according to [10] and are listed in Fig. 2. For this purpose, the maximum tensile strengths according to [29] are considered.

The pinion differs geometrically from the wheel; for the same normal module, the gear has two more teeth, resulting in a larger pitch circle diameter and larger tip circle diameter (see Table 2). The larger dimensions increase the cutting line length, the v-ring length, and the component face area. The cutting force depends on the cutting line length and increases with increasing length. To achieve the same contact pressures of the die-side v-ring and the counterpunch as with the pinion, the corresponding forces must be selected higher. When manufacturing the specimens with the geometry of the pinion, a v-ring on the blankholder is omitted, based on the findings of Nuernberger et al., whereby only a minor influence of blankholder-sided v-rings on the qualities of the produced components was observed [30]. The cutting speed is set at $v = 50$ mm/s for all tests, and the cutting edge radii are also kept the same for both geometries. The punches remained sharp, only the exposed areas in the region of the tooth tips are rounded off with 50 μm to prevent breakout of the cutting edges. The die clearance u_{rel} is kept constant all around and is 0.5% of the sheet thickness. The v-ring cross-sections used can be seen in Fig. 2. The distance between the ring teeth and the tip circle diameters is 3 mm. A special fineblanking oil is used for all fineblanking tests.

4.3 Investigated gear geometry

The geometry of the gearing is chosen based on the limitations of the fineblanking process and process parameters including the fineblanking press as well as available fatigue testing rigs such as the back-to-back running test rigs for future investigations of the pitting strength. Furthermore, the gearing should fail only due to pitting damage in the running tests. The main geometry of this gearing is shown in Table 2. This gear geometry was tested in the past in the research project FVA 453 I [31] with larger facewidth and of the case-carburized material 16MnCr5 regarding pitting damage.

4.4 Investigated gear variants

The pinions and wheels are fineblanked out of 6 mm sheet metal of the materials S355MC and S500MC, whereby no additional mechanical refinishing steps were performed. An exemplary photo of the pinion of each variant is shown in Fig. 3.

For the gears made out of S500MC, an additional variant is created in which the residual stresses are relieved by

Table 1 Chemical constituents in mass percent of an analysis performed with a spark emission spectrometer

denomination	C	Si	Mn	P	S	Al	Nb	Ti	V
S355MC DIN EN 10149-2	Max	Max	Max	Max	Max	Min	Max	Max	Max
	0.12	0.5	1.5	0.025	0.02	0.015	0.09	0.15	0.2
S355MC determined	0.075	0.027	0.506	0.007	0.002	0.03	0.016	0.001	0.007
S500MC DIN EN 10149-2	Max	Max	Max	Max	Max	Min	Max	Max	Max
	0.12	0.5	1.7	0.025	0.015	0.015	0.09	0.15	0.2
S500MC determined	0.074	0.0275	1.650	0.011	0.003	0.023	0.014	0.001	0.049

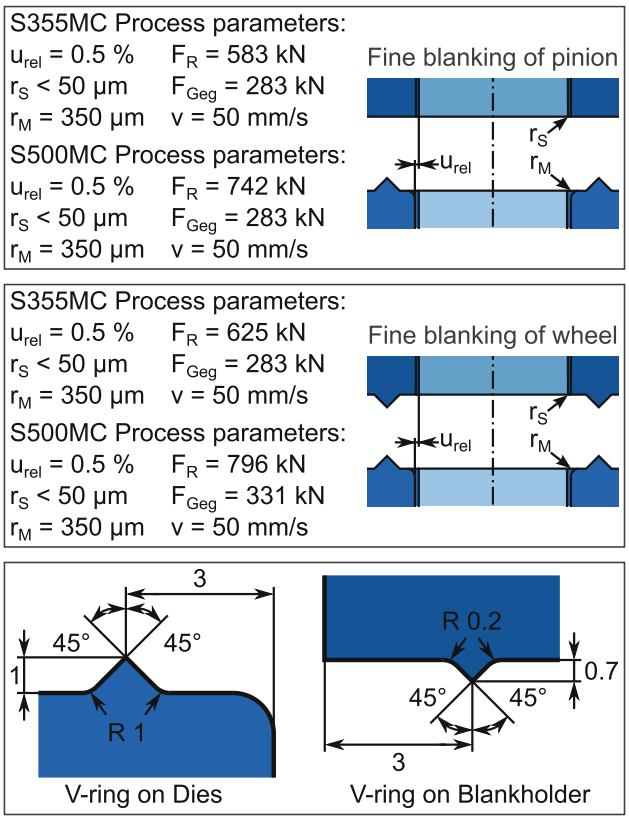

Fig. 2 Process parameters for the two materials and gears

heat treatment. The stress-relieved variant is referred to as S500MC (GG) in the following. With this variant, the influence of the residual stresses on the load-carrying capacity is further investigated. The gears for the variant S500MC (GG) are kept at 540°C for 20 min. Heating is performed at 141Kh^{-1} and cooling without active cooling at 45Kh^{-1}.

4.5 Measurement equipment

4.5.1 Tactile surface measurement

Table 2 Main gear geometry of the investigated gearing

Denomination	Symbol	Pinion	Wheel
Number of teeth	z_1, z_2	23	25
Normal module	m_n	3.0 mm	
Center distance	a	75.6 mm	
Normal pressure angle	α_n	20°	
Helix angle	β	0°	
Facewidth	b	6 mm*	
Profile shift coefficient	x_1, x_2	0.72	0.68
Tip diameter	da_1, da_2	78.3 mm	84.5 mm

*Adjusted for the herein investigated fineblanked gears

Fig. 3 Photo of a pinion of each variant

For the measurement of the cut surface characteristics, a MarSurf XC20 is used, which achieves a resolution of less than 0.5 μm with a probe arm length of 350 mm. To ensure the repeatability of the measurements on the samples, a fixture as shown in Fig. 4 is used. With this device, it was possible to position the wheel or pinion. By using one of the six off-center holes, the pinion or the wheel can be uniquely positioned for the measurements, depending on which measuring point was desired. The measuring device was manufactured with a production tolerance of ± 10 μm. For each geometry and material, four measurements are taken on five specimens for each measurement location on the tooth tip, flank, and tooth root rounding (n=20).

4.5.2 Hardness testing

The hardness measurements are carried out with a LECO AMH-43 hardness tester for the small load range (HV 0.2) according to DIN EN ISO 6507-1 with a test load of 1961 N. For this purpose, as shown in Fig. 5, the specimens are cut

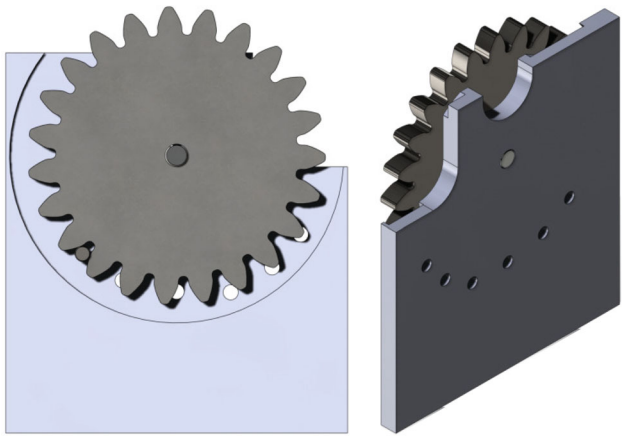

Fig. 4 Device for repeatable measurements at the same measurement location

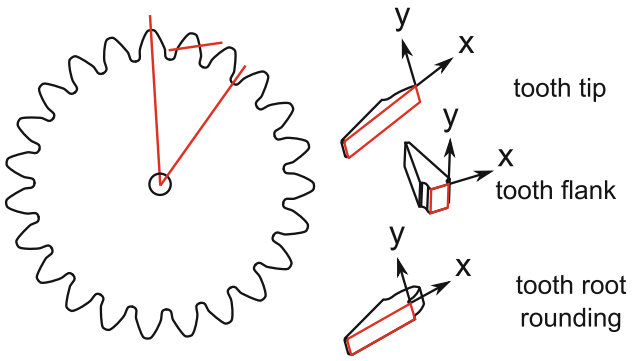

Fig. 5 Schematic illustration of hardness specimens

out of the gears at the three measuring locations (tooth tip, tooth flank, and tooth root fillet) perpendicular to the outer geometry and then polished. When preparing the specimen, heating of the materials' surface and possible falsification of the measurements are minimized by appropriate cooling and low feed rates.

4.5.3 X-ray diffractometer

The surface residual stresses at the flank are measured with a Seifert XRD 3003 PTS x-ray diffractometer system with Cr-Kα radiation. A 1-mm collimator is used and positioned in the middle of the sheet thickness, i.e., the middle of tooth facewidth, with 10 mm distance between the collimator and specimen surface. The residual stresses are evaluated with the $sin^2\Psi$-method.

For the measurements, the tooth is cut with a cutting disk and separated from the gear as shown in Fig. 6. The cutting is performed with sufficient cooling; therefore, influences of the heat on the residual stresses at the tooth flank can be ruled out.

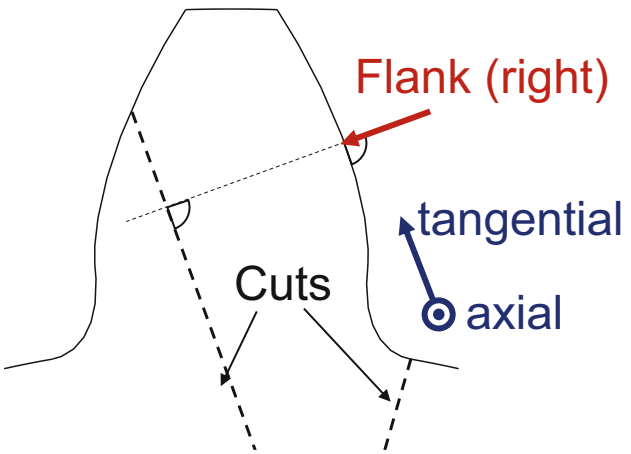

Fig. 6 Preparation of gear and measurement point at the flank

The measurement and preparation were previously described in more detail in [25] and [32].

4.6 Fatigue testing—tooth root bending strength

In this work, standardized fatigue tests regarding tooth root bending strength, i.e., tooth root breakage, in the range of limited life and the endurance strength are carried out. S-N curves for the three different gear variants are determined.

A cost-efficient and commonly used testing method regarding tooth root bending strength of a gear is the testing in a pulsating test rig. The determined strength of the pulsating tests can be transferred to strength numbers for running tests with the conversion factor $f_p = 0.9$ [33]. In addition, the strength numbers standardize the determined load-carrying capacity by considering the influences of the exact geometry and, for example, the roughness in the tooth root to ensure comparable strength numbers.

The testing and evaluation regarding tooth root breakage (tooth root bending strength) are performed in a pulsating test rig according to the standards of FVA Directive 563 I [34]. The teeth of the pinion are loaded with tensile swelling loads at a test frequency of 50 Hz. The lower load limit of the swelling load is 0.3 kN to hold the gear, which is less than 5...10% of the upper load, and therefore, the influence of the clamping force on the test results is negligible [34]. The test gears are symmetrically clamped over $k = 4$ teeth between two plane-parallel jaws as shown in Fig. 7.

The nominal tooth root stress σ_{F0} is calculated according to the standards DIN 3990-3 and ISO 6336-3 [35] as shown in Fig. 7. Hereby, the nominal tooth root stress is calculated, for example, based on the stress correction factor Y_S and the form factor Y_F that are determined from measurements of the gear geometry with contour scans.

To identify the tooth root bending strength number the endurance limit has to be determined. For the standard test procedure, there is a maximum number of load cycles of 6 million, which has to be reached in order to classify the test as passed in the high cycle fatigue regime. In addition, tests

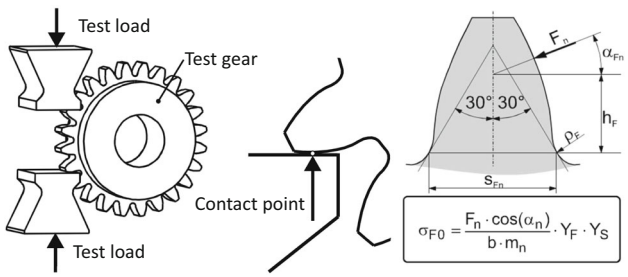

Fig. 7 Clamping of the gear in the pulsating test rig and calculation of nominal tooth root stress σ_{F0} according to ISO 6336-3 and DIN 3990. [36]

are carried out in the limited lifetime on two load stages to determine the S-N curve for 50% failure probability.

With Eq. 1, the nominal strength number $\sigma_{F\,lim}$ for bending is calculated based on the manufactured pinion (factors shown in Table 3) and the determined endurance limit for 50% failure probability $\sigma_{F0\infty,50\%,pulsator}$. The relative notch sensitivity factor $Y_{\delta relT}$ and the relative surface factor Y_{RrelT} are factors depending on the properties of the gear, as well as the stress correction factor Y_{ST} and the size factor Y_X that takes into account the gear size compared to a module 5 mm standard reference gear. For the conversion from 50% failure probability to 1% failure probability, the factor $f_{1\%F}$ is applied [37]. The life factor Y_{NT} is set to 1.0 according to ISO 6336-3 [35].

$$\sigma_{F\,lim} = \frac{\sigma_{F0\infty,50\%,pulsator} \cdot f_P \cdot f_{1\%F}}{Y_{\delta relT} \cdot Y_{RrelT} \cdot Y_{NT} \cdot Y_X \cdot Y_{ST}} \tag{1}$$

For the calculation of the allowable stress number for bending, Eq. 2 is used.

$$\sigma_{FE} = Y_{ST} \cdot \sigma_{F\,lim} \tag{2}$$

With the strength numbers $\sigma_{F\,lim}$ and σ_{FE}, it is possible to compare the material strength of different gears reliably without influences of, e.g., the gear geometry. The influence of the residual stresses is not considered in the strength numbers; consequently, gears of identical materials with different residual stresses usually lead to different strength numbers that show the influence of the residual stresses on the tooth root bending strength.

5 Results

5.1 Cut surface characteristics

Figure 8 shows the cutting surface characteristics of the fineblanked pinions and wheels made from the materials S355MC and S500MC. The die roll and the clean cut are related to the sheet thickness of 6 mm, while absolute values are shown for the angle of clean cut and the burr height. Furthermore, the respective standard deviations are plotted below the mean values given. From the results shown in Fig. 8, a dependence of the clean-cut percentage and the die roll with regard to the cutting line geometry becomes clear. The clean cut has the lowest values at the tooth tip. At the measuring point on the tooth flank, the clean-cut percentage increases compared to that at the tooth tip. For all fineblanked gears, the clean-cut percentages are highest at the root fillet, and consequently, since no fractures or cracks are detected at the measuring points, the die roll heights are lowest. When looking at the clean-cut portions, it is noticeable that, particularly at the tooth tip, the higher strength material S500MC leads to lower edge indentations and thus to increased clean-cut percentages than the material S355MC. The clean-cut angles at the tooth tip and tooth flank are approximately the same distance from the ideal of 90°. The clean-cut angles recorded in the tooth root fillet are on average below the level of the tooth tip and tooth flank. The burr heights at the tooth tip, which are significantly increased compared to the other measuring points for the two materials and gear geometries, are notable. One reason for this is the rounding intentionally applied to the punch in the tooth tip area. The radius creates additional volume, which is filled with material during the fineblanking process and is available for burr formation. This

Table 3 Calculation factors for nominal tooth root stress, nominal stress number (bending), and allowable stress number

Denomination	Symbol	S355MC	S500MC and (GG)
Gear tested over (number of teeth)	k	4	
Load direction angle	α_{Fn}	23.55°	
Bending lever arm	h_{Fn}	3.25 mm	3.08 mm
Tooth root chord at the critical section (30°-tangent)	s_{Fn}	6.73 mm	6.82 mm
Tooth root radius at the critical section (30°-tangent)	ρ_F	1.29 mm	1.35 mm
Roughness	Rz	4.7 µm	6.2 µm
Tooth form factor*	Y_F	1.26	1.16
Stress correction factor*	Y_S	2.22	2.25
Conversion factor $F_{Pn} \rightarrow \sigma_{F0}$ *	C	0.146/mm^2	0.136/mm^2
Conversion factor from 50 to 1% failure probability	$f_{1\%F}$	0.92	
Stress correction factor	Y_{ST}	2.0	
Life factor	Y_{NT}	1.0	
Size factor	Y_X	1.0	

*Valid for the herein selected pulsator clamping

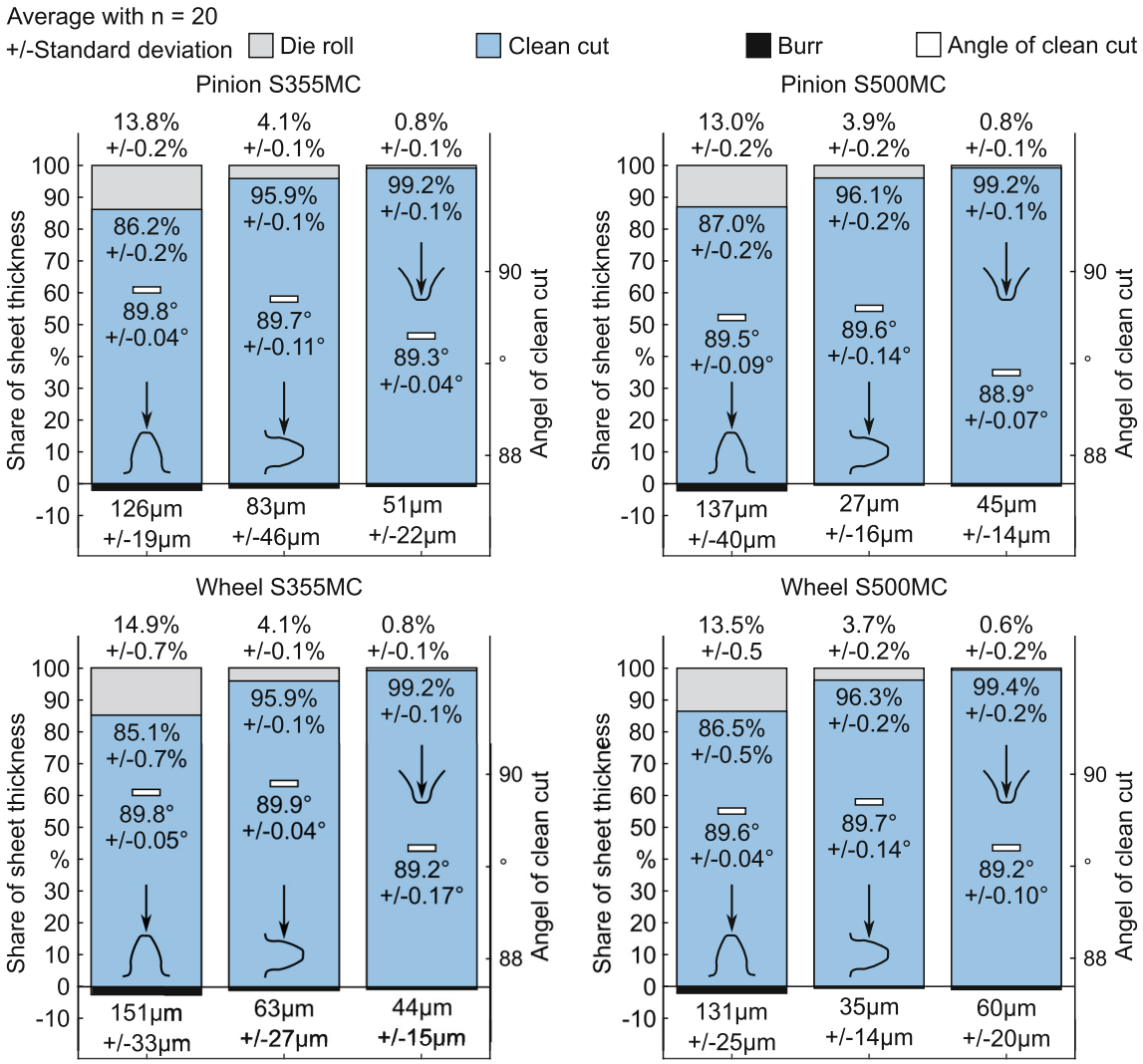

Fig. 8 Cut surface parameters of pinion and wheel made of S355MC (left) and S500MC (right)

material is missing on the die roll side, which additionally favors high-edge feeds at this point [5]. The burr heights at the gears fluctuate more strongly compared to the other cutting surface parameters. The fineblanking process can be partly responsible for this. A falling stamped strip, which adheres to the blankholder due to lubricating oil, is able to damage or deform the burr, which then has a significant effect on the measurement results.

5.2 Hardness

The results of the hardness measurements for the pinion and the gear of the two materials used are shown in Fig. 9. In addition, Fig. 9 shows the results of the hardness measurements for the pinion made of S500MC (GG), which was subjected to heat treatment after fineblanking, ref. Section 4.4. The line type indicates the measuring point and the line color is the distance from the cutting line. When looking at Fig. 9, it is initially noticeable that, apart from the outlier at the tooth root fillet, the measured values for the gear made of S500MC indicate a higher basic hardness at the higher strength material. The hardness values tend to decrease for both gear geometries, materials, and measuring points in the direction of the interior of the component, starting from the cutting surface. When looking at the measured values for the pinion from the two materials, it appears as if the higher base hardness could be exploited to achieve higher hardening near the functional fineblanked surface. The wheels made of S355MC and S500MC show a different performance. The measuring point at the tooth root shows very high hardening for the material S355MC, especially at the distance $x = -0.125$ mm, which is not exceeded even by the higher base hardness. A clear trend with regard to the influence of cutting line geometry and material cannot be determined. Attention must also be paid

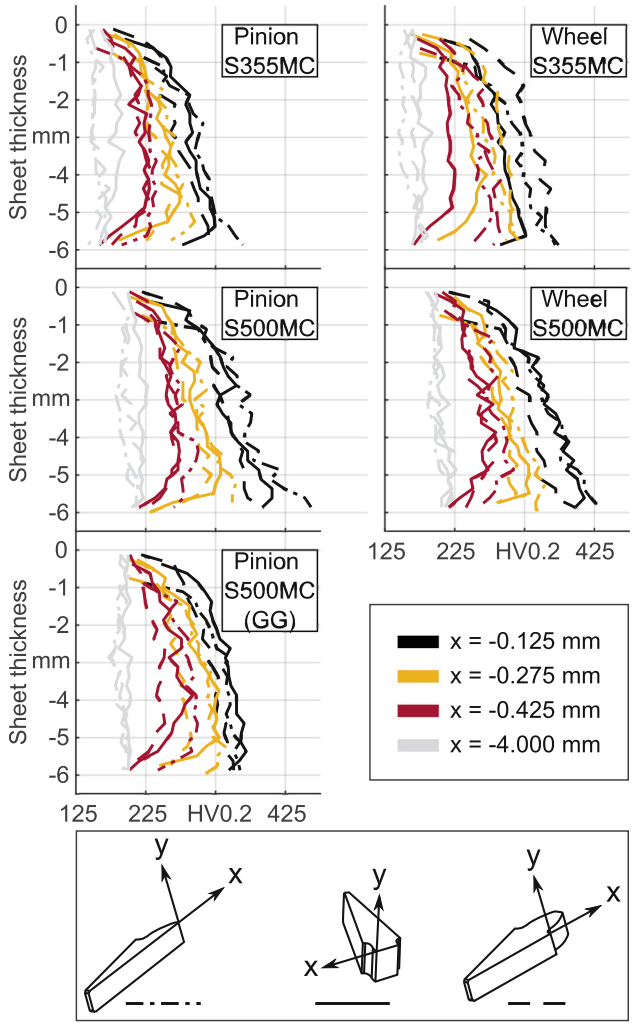

Fig. 9 Cut surface hardness measurements

to the fact that deviations from the ideal cut line during specimen preparation lead to the measurement of a projection and that any inclusions, carbides, cavities, or the supporting effect of the material may influence the hardness values. However, it can be stated that for both materials, very high hardness increases could be achieved by the fineblanking process compared to the present base hardness. The hardness measurements for the stress-relieved pinion made from S500MC (GG) show slightly lower hardness values in the vicinity of the cutting surface ($x = -0.125$ mm), but otherwise, the hardness values are comparable with the untreated variant. If it is assumed that the hardness value is influenced not only by strain hardening but also by residual stresses, the downstream stress relief heat treatment could explain the lower hardness values.

5.3 Residual stresses

The surface residual stresses are measured at the tooth flank near the pitch point of the different fineblanked pinions and wheels. The compressive residual stresses at the flank are usually comparable to the residual stresses in the tooth root for the herein investigated fineblanking process [25].

Figure 10 shows the results of the residual stress measurements. The variants show comparable compressive residual stresses in axial and tangential direction. For the pinions, the residual stresses on both flank sides are shown. The slight, observable differences can be assumed to be due to the scatter of the measurement.

For the material S355MC, the tangential and axial stresses are comparable within approximately $-390\,\mathrm{N/mm^2}$ and $-530\,\mathrm{N/mm^2}$ for the pinions at the left and right flank as well as the wheels. Only the measured wheels made of S500MC show higher compressive residual stresses of up to $-700\,\mathrm{N/mm^2}$ in tangential direction.

In contrast, the pinions made of S500MC show lower compressive residual stresses than the wheels made of S500MC as well as the gears made out of S355MC. Additional measurements for the pinions and wheels confirmed the results shown. An explanation of this based on differences in the investigated properties such as hardness or cut surface characteristics could not be found. For clarification, further residual stress measurements are to be carried out in the first step in order to determine the scatter of the measurements more precisely.

The stress-relieved gears of the variant S500MC (GG) show near zero residual stresses as expected.

5.4 Load-carrying capacity—tooth root bending strength

For the slope of the S-N curve in the limited lifetime, tests on two load stages are carried out. The two load stages are determined on the basis of the number of load cycles achieved. For the determination of the endurance strength, tests on 3–4 load stages are carried out with the top load stage with only

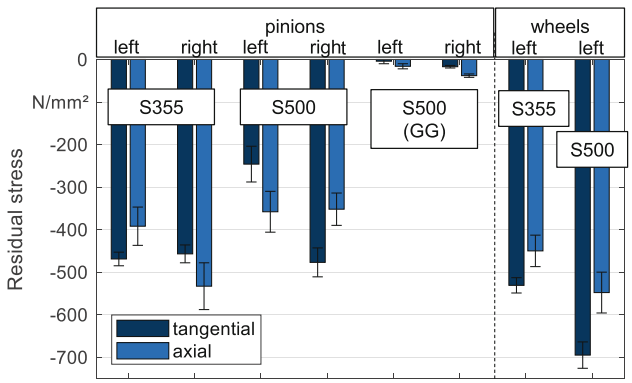

Fig. 10 Results of surface residual stress measurements at the right and left tooth flank of the pinion and wheel of S355MC and S500MC and the stress-relieved variant of S500MC(GG)

failures and the lowest load stage with only passed tests. The load stages for all variants are shown in Table 4. In total, 9–12 tests are performed to determine the endurance limit of each variant.

The results of the tooth root bending strength tests are shown in Fig. 11. All observed tooth root breakages initiate at the surface and in the area of the 30°-tangent in the tooth root as expected. After 6 million load cycles with no failure, the load cycle limit is reached.

S-N curves for 50% failure probability for the fineblanked gears with die radius $r_M = 350\mu m$ of the material S355MC and S500MC, as well as the annealed variant S500MC (GG), are shown in comparison in Fig. 11.

For the S500MC variant, the highest endurance strength of σ_{F0} = 1030 N/mm^2 is determined, followed by the S355MC variant with σ_{F0} = 877 N/mm^2 and the variant S500MC (GG) with σ_{F0} = 792 N/mm^2. The slope in the limited lifetime of the S500MC variants are with $k_{50\%}$ = 3.8 and $k_{50\%}$ = 3.9 comparable. For the S355MC variant, the tooth root breakages near the endurance limit occur comparably later. Breakage even occurred at 5.8 million load cycles. This results in a flatter slope of $k_{50\%}$ = 10.4 in the limited lifetime for the variant S355MC. This corresponds well with the investigations of S355MC with different smaller die edge radii where slopes of 9.9...10.8 were observed [26]. The slope of the S-N curve appears to be independent from the geometry or the observed residual stresses but depends strongly on the material. For case carburized and shot peened gears with higher residual stresses in [1], also, a flatter slope was observed compared to unpeened variants with lower residual stresses.

The results of the calculated strength numbers (acc. to ISO 6336) are shown in Table 5.

Fineblanked gears of S355MC were previously investigated in [26] for a module 4.5 mm gear. Four variants were investigated with different die edge radii $r_M = 50...200\,\mu m$. The fatigue test results showed stress numbers within σ_{Flim} = 318…327 N/mm^2 correlating with the die edge radii.

The herein-determined stress numbers as well as the stress numbers previously determined in [26] are shown in Fig. 12 in comparison. For the surface hardness, the maximum measured hardness in the tooth root is used.

For the herein-investigated gears, the larger die edge radius of $r_M = 350\,\mu m$ leads to a higher fatigue limit

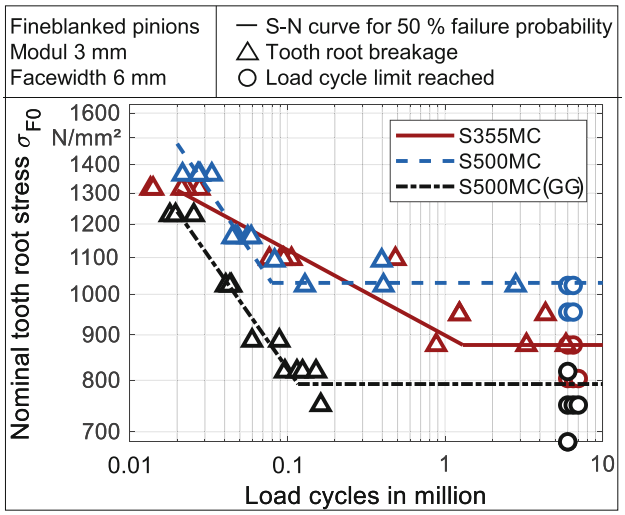

Fig. 11 S-N curve for tooth root breakage for 50% failure probability of the module 3 mm fineblanked gear variants with the materials S355MC, S500MC, and S500MC (GG)

compared to the variants with smaller die edge radii for S355MC of previous research [26]. The annealed variant S500MC (GG) is roughly on the same level but with higher surface hardness. For the S500MC variant, the highest fatigue limit is observed but also the highest surface hardness.

These determined strength numbers can be compared to test results of reference gears stated in ISO 6336-5 [38]. Compared to wrought normalized low carbon steels that have strength numbers of $\sigma_{Flim} = 120...230\,N/mm^2$, these fineblanked gears have a significantly higher tooth root bending strength. The fineblanked gear variant S500MC would correspond well within the numbers for case-carburized gears with $\sigma_{Flim} = 310...550\,N/mm^2$, especially with gears in unpeened condition which typically show strength numbers in the range of $\sigma_{Flim} = 300...420\,N/mm^2$ [39].

The stress numbers for bending are determined for the pinions. The pinions of S355MC show comparable results to the variants of the same material determined previously for module 4.5 mm gears. By comparing all variants made of S355MC, it is clear that the fatigue limit correlates with the die edge radius as well as the residual stresses caused by it.

The pinions of S500MC show slightly lower compressive residual stresses than the pinions of S355MC, whereas the S500MC (GG) pinions have no residual stresses but

Table 4 Pulsator testing load stages

Denomination	Limited lifetime	Endurance strength
S355MC	9.0/7.5 kN	5.5/6.0/6.5 kN
S500MC	10.0/8.5 kN	7/7.5/8.0 kN
S500MC (GG)	9.0/7.5 kN	5.0/5.5/6.0/6.5 kN

Table 5 Results of fatigue tests—tooth root bending stress numbers

Symbol	S355MC	S500MC	S500MC (GG)
σ_{FE}	703	836	643
σ_{Flim}	352	418	322

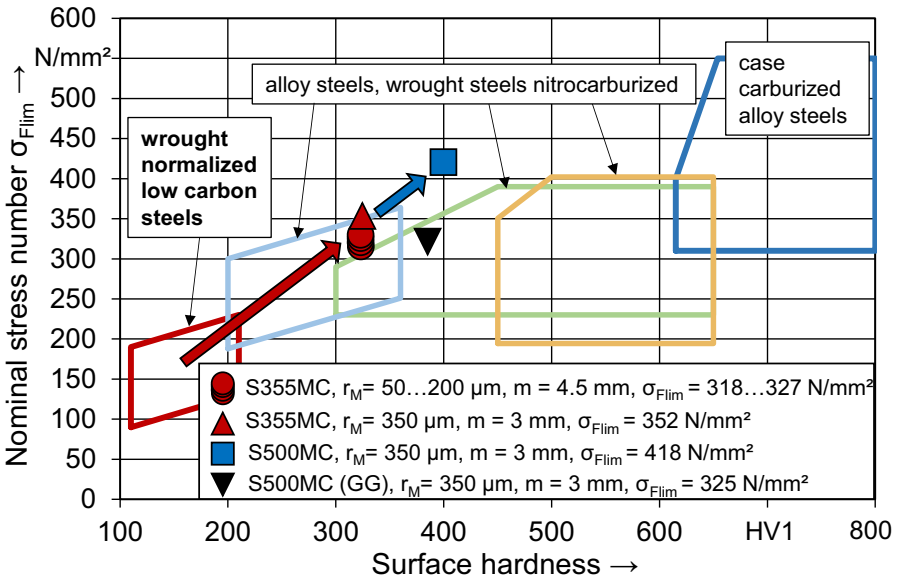

Fig. 12 Nominal and allowable stress numbers (bending) acc. ISO 6336-5 for the module 3 mm gears of S355MC, S500MC, and annealed S500MC (GG) in comparison to previous results of module 4.5 mm gears of S355MC with smaller die edge radii [26]

comparable hardness as the S500MC variant. Despite the slightly lower residual stresses in the pinions of S500MC, the higher strength material results in a significantly higher fatigue limit.

6 Conclusion

Pinions and wheels of module 3 mm were manufactured by fineblanking using S355MC and S500MC. The fineblanking process parameters are selected in such a way that the compressive residual stresses are as high as possible. The cut surface that is the functional surface of the gears is investigated regarding its properties such as, e.g., the amount of clean cut. For the higher-strength steel S500MC, also, a residual stresses free variant is produced by stress relief treatment.

The three investigated variants, S355MC, S500MC, and the annealed S500MC (GG), are in addition investigated with respect to hardness and residual stresses as well as tested regarding tooth root breakage. The bending strength numbers according to ISO 6336 are determined and compared.

With regard to the clean-cut percentage and the die roll of the functional surface, the measured pinions and wheels show a large dependence on the cutting line geometry. The cutting surface parameters for pinions and wheels are quite comparable for both materials investigated and show high clean-cut percentages of over 95.9% at the tooth flank and tooth root. The clean-cut angles for the tooth flank measuring point, which is in the relevant range for the use of gears, are close to the ideal of 90°. In addition, the fineblanking process achieved a high degree of hardening in the area of the functional surface compared with the hardness of the base materials.

The process parameters for the fineblanking of S355MC steel investigated in previous works were transferred to the higher-strength material S500MC. High compressive residual stresses could be achieved in the fineblanked gears.

The tooth root bending strength could be further increased with a larger die edge radius and higher strength material compared to previous results.

For the higher-strength material, higher compressive residual stresses are induced only at the wheels. The reason is still the subject of ongoing investigations. However, the tested pinions still show a significantly higher tooth root bending strength ($\sigma_{Flim} = 418\,N/\mathrm{mm}^2$) than the tested pinions made of S355MC ($\sigma_{Flim} = 352\,N/\mathrm{mm}^2$).

The pinions made of S500MC with stress relief treatment show near zero residual stresses without significant change in hardness. The bending strength is significantly lower ($\sigma_{Flim} = 322\,N/\mathrm{mm}^2$).

Tooth root bending strength numbers comparable to unpeened case-carburized gears are achieved for the herein-investigated fineblanked gears.

In the next step, the flank load-carrying capacity, i.e., pitting strength, is determined for the three variants. In the course of this, further properties of the gears, such as the gear quality, are also to be investigated.

Author Contributions All authors contributed to the study conception and design. Material preparation, data collection, and analysis were performed by Anian Nürnberger and Daniel Müller. The first draft of the manuscript was written by Anian Nürnberger] and Daniel Müller, and all authors commented on previous versions of the manuscript. All authors read and approved the final manuscript.

Funding Open Access funding enabled and organized by Projekt DEAL. This work is funded by the Deutsche Forschungsgemeinschaft (DFG, German Research Foundation)-project number 374524261 - VO 1487/30-1; VO 1487/30-2; VO 1487/30-3; STA 1198/13-1; STA 1198/13-2; STA 1198/13-3 and is part of the DFG-priority program "Target Use of Forming Induced Residual Stresses in Metal Components (SPP2013)."

Availability of data and material Not applicable

Code Availability Not applicable

Declarations

Ethics approval Not applicable

Consent to participate Not applicable

Conflict of interest The authors declare no competing interests.

References

1. Güntner C, Tobie T, Stahl K (2017) AGMA 2017 Fall Technical Meeting, chapter Influences of the residual stress condition on the load carrying capacity of case hardened gears. Columbus, Ohio, USA, pp 328–344
2. Winderlich B (1990) Das konzept der lokalen dauerfestigkeit und seine anwendung auf martensitische randschichten, insbesondere laserhärtungsschichten. eng.: The concept of local fatigue strength and its application to martensitic boundary layers. Materialwissenschaft und Werkstofftechnik 21(10):378–389, ISSN 0933-5137
3. Birzer F (1996) Feinschneiden und Umformen Wirtschaftliche Fertigung von Präzisionsteilen aus Blech. Moderne Industrie, Landsber/Lech. ISBN 3478931541
4. Zheng Q, Zhuang X, Zhao Z (2019) State-of-the-art and future challenge in fine-blanking technology. Production Engineering 13(1):61–70 ISSN 0944-6524
5. Demmel P, Nothhaft K, Golle R, Hoffmann H (2012) Zerteilen. In Hoffmann H, Neugebauer R, Spur G (eds) Handbuch Umformen, Edition Handbuch der Fertigungstechnik / hrsg. von Günter Spur, pp 679–729. Hanser, München, ISBN 3446427783
6. Dietrich J (2018) Praxis der Umformtechnik. Springer Fachmedien Wiesbaden, Wiesbaden. ISBN 978-3-658-19529-8
7. Klocke F (2017) Fertigungsverfahren 4. Springer, Berlin Heidelberg, Berlin, Heidelberg. ISBN 978-3-662-54713-7
8. GmbH Schuler (1996) Handbuch der Umformtechnik. Springer, Berlin and Heidelberg. ISBN 978-3-662-07704-7
9. VDI 2906 Blatt 5, (2013) Schnittflaechenqualitaet beim Schneiden. Beuth Verlag, Berlin, Brechen und Lochen von Werkstücken aus Metall Feinschneiden
10. Schmidt R-A (2006) Umformen und Feinschneiden. Carl Hanser Fachbuchverlag, s.l., 1. aufl. edition, ISBN 3446409645. http://www.hanser-elibrary.com/isbn/9783446409644
11. Kim JD, Kim HK, Heo YM, Chang SH (2011) A study on the relation between die roll height and die chamfer shape in fine blanking for special gear. Advanced Materials Research 320:92–96
12. VDI 3345, (1980) Feinschneiden. VDI-Verlag GmbH, Düsseldorf
13. Fuchiwaki K, Mure Y, Yoshida K, Murakawa M (2017) Prediction of die-roll in fine blanking by use of profile parameters. Procedia Engineering 207:1564–1569 ISSN 18777058
14. Kim JD (2013) An experimental study on the effect of die chamfer shape and v-ring position on die roll height in the fine blanking of a special part with various corner shapes. Applied Mechanics and Materials 365–366:569–575
15. Aravind U, Chakkingal U, Venugopal P (2021) A review of fine blanking: influence of die design and process parameters on edge quality. Journal of Materials Engineering and Performance 30(1):1–32 ISSN 1059-9495
16. Spišák E, Majerníková J, Spišáková E (2015) The influence of punch-die clearance on blanked edge quality in fine blanking of automotive sheets. Materials Science Forum 818:264–267
17. Sahli M, Roizard X, Assoul M, Colas G, Giampiccolo S, Barbe JP (2021) Finite element simulation and experimental investigation of the effect of clearance on the forming quality in the fine blanking process. Microsystem Technologies 27(3):871–881 ISSN 0946-7076
18. Thipprakmas S (2009) Finite-element analysis of v-ring indenter mechanism in fine-blanking process. Materials & Design 30(3):526–531 ISSN 02613069
19. Elyasi M (2013) An investigation on the parametric analysis of v-ring indenter mechanism in fine-blanking process. International Journal of Mechanics and Applications 3(4):76–80
20. Thipprakmas S (2011) Improving wear resistance of sprocket parts using a fine-blanking process. Wear 271(9-10):2396–2401 ISSN 00431648
21. Česnik D, Bratuš V, Kosec B, BIZJAK M, (2012) Distortion of ring type parts during fine-blanking. Metalurgija 51:157–160
22. Aravind U, Chakkingal U, Venugopal P (2019) Investigation of a modified fine piercing process on extra deep drawing grade steel. Journal of Materials Engineering and Performance 28(12):7789–7803 ISSN 1059-9495
23. Stahl J, Müller D, Tobie T, Golle R, Volk W, Stahl K (2019a) Residual stresses in parts manufactured by near-net-shape-blanking. Production Engineering 13(2):181–188 ISSN 0944-6524
24. Stahl J, Müller D, Pätzold I, Golle R, Tobie T, Volk W, Stahl K (2019b) The influence of residual stresses induced by near-net-shape blanking processes on the fatigue behavior under bending loads. IOP Conference Series: Materials Science and Engineering 651(1):012086 ISSN 1757-8981
25. Müller D, Stahl J, Nürnberger A, Golle R, Tobie T, Volk W, Stahl K (2021a) Shear cutting induced residual stresses in involute gears and resulting tooth root bending strength of a fineblanked gear. Archive of Applied Mechanics 91(8):3679–3692 ISSN 0939-1533
26. Müller D, Stahl J, Nürnberger A, Golle R, Tobie T, Volk W, Stahl K (2021b) Einfluss von prozessinduzierten Eigenspannungen auf die Zahnfußtragfähigkeit schergeschnittener Zahnräder. Forschung im Ingenieurwesen 85(3):709–721 ISSN 0015-7899
27. DIN Deutsches Institut für Normung e. V. (2013a) Warmgewalzte Flacherzeugnisse aus Stählen mit hoher Streckgrenze zum Kaltumformen – Teil 2: Technische Lieferbedingungen für thermomechanisch gewalzte Stähle
28. Deutsches Institut DIN, für Normung e. V. (2013) Warmgewalzte Flacherzeugnisse aus Stählen mit hoher Streckgrenze zum

Kaltumformen - Teil 1: Allgemeine technische Lieferbedingungen. Deutsche Fassung EN 10149–1:2013
29. DIN EN 10149-2 (1995) Hot rolled flat products made of high yield strength steels for cold forming
30. Nürnberger A, Müller D, Martinitz L, Hartmann C, Tobie T, Stahl K, Volk W (2022) Comparative study of v-ring indenter configurations in fineblanking in order to derive tool design guidelines. The International Journal of Advanced Manufacturing Technology 123(11): 4171–4179. ISSN 1433-3015. DOIurlhttps://doi.org/10.1007/s00170-022-10345-6
31. Schwienbacher S, Wolter B, Tobie T, Höhn B-R, Kröning M (2007) FVA 453 I: Randzonentragfähigkeit - Zahnflanke: Ermittlung und Charakterisierung von Randzonen-Kennwerten und -eigenschaften und deren Einfluss auf die Flankentragfähigkeit einsatzgehärteter, geschliffener Zahnräder. eng.: Determination and characterization of surface region properties and their influence on flank load carrying capacity. (830)
32. Stahl J, Müller D, Tobie T, Golle R, Volk W, Stahl K (2018) Production Engineering, chapter Residual stresses in parts manufactured by near-net-shape-blanking. Springer, Dec 2018
33. Dobler F, Tobie T, Stahl K (2015) Influence of low temperatures on material properties and tooth root bending strength of case-hardened gears. In: ASME 2015 Power Transmission and Gearing Conference; 23rd Reliability, Stress Analysis, and Failure Prevention Conference. vol 10 ASME, Sunday 2 August 2015. ISBN 978-0-7918-5720-5
34. Tobie T, Matt P (2012) FVA directive 563 I: Standardisation of load capacity tests
35. ISO 6336-3 (2019) Calculation of load capacity of spur and helical gears: calculation of tooth bending strength
36. Höhn B-R, Oster P, Michaelis K, Suchandt T, Stahl K (2000) Bending fatigue investigation under variable load conditions on case-carburized gears. AGMA 2000 Fall Technical Meeting
37. Rettig H (1987) Ermittlung von Zahnfußfestigkeits-Kennwerten auf Verspannungsprüfständen und Pulsatoren. eng.: Determination of Tooth root strength values on back-to-back test rigs and pulsators. Antriebstechnik 26(2):51–55
38. ISO 6336-5(2016) Calculation of load capacity of spur and helical gears: strength and quality of materials
39. Weigand U (1999) Werkstoff- und Wärmebehandlungseinflüsse auf die Zahnfußtragfähigkeit. PhD thesis, Technische Universität München